

KfK 3284

Juli 1982

**A Study of Some Numerical
Problems for SIMMER-II Fluid
Dynamics Related to the
Postdisassembly Expansion
Phase for an LMFBR
Unprotected Loss-of-Flow
Accident**

P. Schmuck

Institut für Neutronenphysik und Reaktortechnik
Projekt Schneller Brüter

Kernforschungszentrum Karlsruhe

KERNFORSCHUNGSZENTRUM KARLSRUHE

Institut für Neutronenphysik und Reaktortechnik
Projekt Schneller Brüter

KfK 3284

A Study of Some Numerical Problems for SIMMER-II Fluid
Dynamics Related to the Postdisassembly Expansion Phase
for an LMFBP Unprotected Loss-of-Flow Accident

P. Schmuck

Kernforschungszentrum Karlsruhe GmbH, Karlsruhe

Als Manuskript vervielfältigt
Für diesen Bericht behalten wir uns alle Rechte vor

Kernforschungszentrum Karlsruhe GmbH
ISSN 0303-4003

A Study of Some Numerical Problems for SIMMER-II Fluid Dynamics Related to the Postdisassembly Expansion Phase for an LMFBR Unprotected Loss-of-Flow Accident

Abstract

Using a test problem reflecting important characteristics of the post-disassembly expansion phase some numerical problems of SIMMER-II fluid dynamics are studied. The one-dimensional test problem considers the expulsion of a liquid slug by an expanding gas. SIMMER-II solutions for different mesh sizes are compared to the exact solution. The following conclusions can be drawn for SIMMER-II solutions:

- (1) The smearing of the gas/liquid interface is caused mainly by the upwind (donor cell) differencing used in SIMMER-II. The von Neumann formula represents this smearing very well, therefore only a weak dependence on the mesh size is observed.
- (2) The gas velocities do not agree very well with the exact solution. They depend strongly on the mesh size. A smaller mesh size infers initially a worse solution.
- (3) The gas pressures are too low, mainly in the smeared interface region. At the front of this region they decrease sharply, causing too high velocities.
- (4) The kinetic energy of the liquid slug agrees well with the exact value; only in the initial phase of the expansion a larger discrepancy related to a special SIMMER-II algorithm is observed.

Eine Untersuchung von numerischen Problemen der Fluidodynamik von SIMMER-II für die Postdisassemblyexpansionsphase eines Kühlmitteldurchsatzstörfalls in einem natriumgekühlten schnellen Brutreaktor

Zusammenfassung

Anhand eines Testbeispiels wird die für die Postdisassembly-Phase typische Verdrängung einer Flüssigkeit durch eine sich ausbreitende Gasströmung diskutiert. Für die mit SIMMER-II berechneten Lösungen zeigt sich, daß

- (1) die Verschmierung der Grenzfläche gas/flüssig im wesentlichen durch das verwendete Aufwind-Differenzenverfahren zustande kommt und sehr gut durch die von Neumann-Formel dargestellt werden kann (d. h. unter anderem, daß die Verschmierung nur schwach von der Maschenweite abhängt);
- (2) die Gasgeschwindigkeiten relativ schlecht mit der exakten Lösung übereinstimmen und stark von den verwendeten Maschenweiten abhängen (wobei eine kleine Maschenweite am Anfang ungünstiger ist);
- (3) die Gasdrücke vor allem in der verschmierten Grenzfläche zu gering sind und an der Front stark abnehmen (wodurch zu hohe Geschwindigkeiten induziert werden);
- (4) die kinetische Energie der Flüssigkeit i. a. sehr gut mit dem exakten Wert übereinstimmt (nur in der Anfangsphase der Expansion kommt es zu bemerkenswerten Abweichungen, die durch einen speziellen SIMMER-II Algorithmus verursacht werden).

Table of Contents

	page
1. Introduction	1
2. Description of the test problem; Analytical solutions of the model equations by series expansion; Test problem parameters; Self similarity of the solution	3
3. Analysis of finite differencing as used in SIMMER-II hydrodynamics; Von Neumann formula for interface smearing; Application of the Hirt-Zhoukov method to calculate the numerical viscosity	10
4. Discussion of SIMMER-II results and their relation to analytical solutions; Interface smearing; Change of the mass of the liquid slug; Flow field parameters: gas pressures and velocities; Kinetic energy of the liquid slug	17
5. Summary, conclusions and suggestions for future work	26
References	29
Figures 1 - 12	31
Appendix: SIMMER-II input data	43

List of Figures

- Fig. 1 : Geometry of the test problem: initial distribution of gas, liquid and vacuum in a cylindrical tube
- Fig. 2 : Schematic sketch of the velocity distribution of the gas at time t between the liquid slug and the gas masses at rest
- Fig. 3 : Important quantities determining the space dependence of the gas velocity for a uniformly accelerated liquid slug
- Fig. 4 : Axial convection of the gas mass at the mesh interface $j + 1/2$:
a) upwind differencing
b) linearly interpolated differencing
- Fig. 5 : Time development of a step profile in gas density
(mesh size: 6 cm)
- Fig. 6 : Time dependence of a step profile in gas density
(mesh size: 12 cm)
- Fig. 7 : Gas pressure distribution at 100 ms
- Fig. 8 : Gas velocity distribution at 100 ms
- Fig. 9 : Gas pressure distribution at 200 ms
- Fig. 10: Gas velocity distribution at 200 ms
- Fig. 11: Kinetic energy of the liquid slug (analytical solution)
- Fig. 12: Deviation of SIMMER-II results from exact kinetic energy values

1. Introduction

Postdisassembly studies with the SIMMER-II code /1/ have been performed for LMFBRS /11/, /12/. Typical cases showed that the hot core materials (fuel and steel) penetrated the above core structures and entered into the upper sodium plenum. The contact of hot fuel and steel two-phase mixtures with the liquid sodium leads to high heat transfer rates and to sodium evaporation. The pressure generated by the evaporated sodium causes the build-up of a (more or less) semi-spheric bubble in the upper sodium plenum.

It is important to study in some detail the physics of the developing bubble, i.e. the physical processes occurring in the bubble and at the bubble/liquid sodium interface. These processes determine the acceleration of the liquid sodium displaced in the upper sodium plenum and are therefore closely connected with mechanical loads imparted to the reactor tank. The dynamics of the interface can influence the energetics of the bubble expansion process. If instabilities develop at the interface (e.g. Taylor type instabilities) liquid sodium droplets can be formed and enter into the bubble ("entrainment"). These droplets which may have small diameters (and therefore a relatively large surface area) can influence the pressure build-up in various ways. One important process is fuel vapor condensation on the cold droplet surfaces which may transfer quickly the heat content of the vapor to the sodium droplets. As a consequence fuel vapor is lost as a pressure source. But the sodium vapor generated replaces rapidly the fuel vapor and may lead to high vapor pressures also. The heating of the sodium droplets by the contact of liquid fuel and liquid sodium or by the radiation from the hot two-phase mixture represent other interesting possibilities which can have an impact on the pressure source.

In SIMMER-II calculations the structure of the bubble/liquid sodium interface is determined by the models and numerical techniques used in the code. The smearing of the bubble/liquid interface in SIMMER-II calculations, the effects of this smearing on the flow field (i.e. pressures and velocities) and on the kinetic energy of the accelerated, cold liquid are studied in this report quantitatively using a test problem. No heat transfer is accounted for in this test problem, only fluid dynamics effects are

investigated in this first step. Heat transfer effects will generally lead to a better (i.e. sharper) defined interface in SIMMER-II because of the vaporization of the liquid sodium at the interface. These effects are beyond the scope of the present report. However, it is hoped that in follow-up investigations heat transfer and its consequences can also be studied in detail.

2. Description of the test problem

We choose a classical problem of one-dimensional gas dynamics to challenge SIMMER-II numerics for postdisassembly conditions. The situation is shown in Fig. 1 (all figures are located behind the text section). A perfect gas occupies the space $x < 0$ in an infinite cylindrical pipe. The gas space is terminated by a liquid slug at $x = 0$ at time $t = 0$ (cf. Fig. 1). The gas has initially the uniform pressure p_0 . The liquid slug is accelerated into a vacuum space which is extending from the right hand boundary of the slug to infinity. The gas and the liquid slug are at rest initially. The movement starting at $t = 0$ can be described as follows. A rarefaction wave in the gas is formed while the liquid is accelerated. One boundary of this wave moves to the right together with the liquid slug, the other moves to the left into the resting gas with a velocity equal to the velocity of sound in the gas at rest. In the following we formulate the relevant equations and solve them analytically by series expansion for the initial movement. The expansion times considered are typical for postdisassembly expansion in an LMFBR of SNR-300 size.

Analytical solution of the model equations by series expansion

We use the well known gas dynamic equations for one-dimensional movement as given for example by Landau and Lifshitz /2/. Pressure p and density are related to the gas velocity v as follows

$$p = p_0 \left(1 - \frac{1}{2}(\gamma-1) |v|/c_0\right)^{2\gamma/(\gamma-1)} \quad (2.1)$$

$$\rho = \rho_0 \left(1 - \frac{1}{2}(\gamma-1) |v|/c_0\right)^{2/(\gamma-1)} \quad (2.2)$$

where

- p ... gas pressure
- p_0 ... initial gas pressure
- ρ ... gas density
- ρ_0 ... initial gas density
- c_0 ... velocity of sound in gas at rest

$\gamma = c_p/c_v$... ratio of specific heat at constant pressure to
 specific heat at constant volume
 v ... gas velocity

The gas velocity v is generally a complicated function of the spatial coordinate x and the problem time t . However in our test example we can approximate this velocity with high accuracy as will be demonstrated later. Fig. 2 is a schematic picture of the velocity distribution of the gas between the accelerated liquid slug and the unperturbed gas region as calculated from gas dynamics (cf. /2/).

The equation of motion for the liquid slug (i.e. also for the gas/liquid interface) can be written in dimensionless variables as follows:

$$\frac{d\bar{U}}{d\bar{t}} = \left[1 - \frac{\gamma-1}{2} \bar{U} \right]^{2\gamma/(\gamma-1)} \quad (2.3)$$

where

$\bar{U} = U/c_0$... dimensionless slug velocity

$\bar{t} = \frac{tp_0}{mc_0}$... dimensionless problem time

$U(t)$... velocity of the liquid slug

t ... problem time

m ... liquid slug mass per unit area

The velocity of the slug is initially assumed to be zero, i.e. $\bar{U}(\bar{t}=0) = 0$. During the whole acceleration process $\bar{U}(t) = U(t)/c_0 \ll 1$ remains valid. Therefore the expression on the right hand side of equation (2.3) can be developed in a quickly convergent Taylor series.

Using equation (3) we calculate the first three expansion coefficients:

$$\left(\frac{d\bar{U}}{d\bar{t}} \right)_{\bar{t}=0} = 1 \quad (2.4a)$$

$$\left(\frac{d^2\bar{U}}{d\bar{t}^2} \right)_{\bar{t}=0} = -\gamma \left[1 - \frac{\gamma-1}{2} \bar{U} \right]^{\frac{4\gamma}{\gamma-1} - 1} \Big|_{\bar{t}=0} = -\gamma \quad (2.4b)$$

$$\begin{aligned} \left(\frac{d^3\bar{U}}{d\bar{t}^3} \right)_{\bar{t}=0} &= \gamma \left(\frac{3\gamma+1}{2} \right) \left[1 - \frac{\gamma-1}{2} \bar{U} \right]^{\frac{6\gamma}{\gamma-1} - 2} \Big|_{\bar{t}=0} \\ &= \gamma \frac{3\gamma+1}{2} \end{aligned} \quad (2.4c)$$

and therefore

$$\bar{U} = \bar{t} - \frac{\gamma}{2} \bar{t}^2 + \frac{\gamma}{6} \frac{3\gamma+1}{2} \bar{t}^3 - \dots \quad (2.5a)$$

or in dimensional form

$$U = \frac{tp_o}{m} - \frac{\gamma}{2} \frac{p_o^2}{m^2 c_o^2} t^2 + \frac{\gamma}{6} \frac{3\gamma+1}{2} \frac{p_o^3}{m^3 c_o^2} t^3 - \dots \quad (2.5b)$$

Closer inspection shows that the series (2.5) has terms with alternating signs.* Therefore the accuracy of the representation of U can be checked easily /3/. For this check we use the test problem parameters given in the next section. In addition we assume that the maximum time considered is $t = 200$ ms. This leads to the result that the linear term in (2.5) represents U with a maximum error of 0.9 % and the first two terms of (2.5) represent U with a maximum error of 0.01 %. Therefore the third order term in (2.5) is only needed to check the accuracy of the series representation, and not for actual computations of \bar{U} . The representation (2.5) of the piston velocity provides the basis for easy computations of other important quantities. For instance equation (2.5) can be used to calculate the time dependent location of the interface:

$$X = \frac{p_o}{2m} t^2 - \frac{\gamma}{6} \frac{p_o^2}{m^2 c_o^2} t^3 \quad (2.6)$$

* monotonically decreasing

This representation has even smaller maximum errors up to 200 ms compared to the series expansion for the velocity U (2.5). So the first (quadratic) term in (2.6) represents the location of the interface with accuracy higher than 0.6 %.

As the numerics of SIMMER results normally in much larger errors, we will use the linear approximation for the velocity and the quadratic expression for the interface location. An exception will be made only for the calculation of the kinetic energies of the slug where the exceptional high accuracy of SIMMER results demands that two terms in formula (2.5) are used.

We proceed now to calculate the velocity v in the gas behind the piston. Because the deviation from linearity is very low we can use the results of Landau and Lifshitz /2/ for a uniformly accelerated piston $U = at$ with $a = p_0/m$. The gas velocity is then given by

$$v = \left[c_0 + \frac{1}{2} (\gamma+1) at \right] / \gamma - \sqrt{\left\{ \left[c_0 + \frac{1}{2} (\gamma+1) at \right]^2 - 2a\gamma (c_0 t + x) \right\}} / \gamma \quad (2.7)$$

valid in the time interval $t = [0, 2c_0/(\gamma-1)a]$. A schematic picture of the velocity has been given in Fig. 2. As the error in the piston velocity is small (less than 0.9 %) during the time considered (200 ms) it seems reasonable to assume that the error in v is even smaller. The justification for this assumption is as follows. At the right boundary the velocity coincides with the piston velocity. Therefore the error in the gas velocity is taken over directly from piston velocity. At the left boundary ($x = -c_0 t$) the gas velocity v is zero and there should be no additional error generated at this boundary.

The spatial dependence of v is nearly linear as the following consideration shows. In Fig. 3 the typical dependence of the gas velocity v on the space coordinate is depicted. In our cases always

$$\frac{a}{2} t^2 \ll c_0 t \quad (2.8)$$

i.e. $\frac{a}{2} t \ll c_0$ is valid. Therefore the gradient $\frac{\partial v}{\partial x}$ can be calculated from equation (2.6) approximately by

$$\frac{\partial v}{\partial x} \approx \frac{a}{c_o} = \frac{p_o}{mc_o} \quad (2.9)$$

in the interval $[-c_o t, \frac{a}{2} t^2]$. As made plausible by Fig. 3 and indicated by equation (2.9) the gas velocity is only weakly dependent on the coordinate x and this dependence is almost linear.

In section four gas velocities calculated with SIMMER-II will be compared to gas velocities calculated according to equation (2.7). Oscillations appear in the velocities calculated with SIMMER-II, mainly near the gas/liquid interface which suffers numerical smearing. Such oscillating behavior cannot be deduced from equation (2.7) however.

The kinetic energy of the liquid slug is computed by

$$K_E = \frac{m_p U^2}{2} \sim \frac{m_p}{2} \left(\frac{tp_o}{m} \right)^2 \left(1 - \frac{\gamma}{2} \frac{tp_o}{mc_o} \right)^2 \quad (2.10)$$

where

m_p ... total mass of liquid slug

and the other quantities have been explained earlier. The accuracy of expression (2.10) is better than 0.02 % during the initial 200 ms of our test problem. The quadratic term is clearly dominating during this time interval.

The volume displaced by the slug movement is expressed by

$$\Delta V(t) = F \int_0^t U dt' = F \cdot X(t) \quad (2.11)$$

where $X(t)$ is given in (2.6) and F is the total cross section area of the liquid slug. $\Delta V(t)$ shows also a dominating quadratic term in time.

Summarizing the trends of our analytical solutions we may say that our test problem generates a rather prototypic accelerated flow of the gas and the liquid slug. The test problem parameters described in detail below have been chosen carefully to reflect prototypic conditions as well as possible.

Test Problem Parameters

The parameters chosen simulate the postdisassembly conditions in the upper sodium plenum of the SNR-300. The pressure values are prototypical in the sense that such values are typical when a mild fuel-coolant interaction takes place during the fuel discharge to the upper plenum. The following geometrical and physical conditions were chosen:

Mass of sodium slug (m_p)	:	1688.8 kg
Length of slug	:	2.4 m
Cross section of the slug (F)	:	0.101788 m ²
Mass per unit area (m)	:	16591 kg/m ²

Nitrogen gas is used in the gas region with an initial pressure of 6.0255 bar. As nitrogen is a diatomic gas the value of γ is 7/5.

Self-similarity of the solution

Our test problem allows self similar solutions and is governed by few dimensionless parameters. They have been used partially in this section and we collect them for completeness here. Dimensionless quantities are marked with a bar (as done earlier).

$$\text{Time : } \bar{t} = \frac{tp_o}{mc_o} \quad (2.12)$$

$$\text{Velocity : } \bar{U} = \frac{U}{c_o} \quad (2.13)$$

Time and velocity scales lead to a length scale

$$\text{Length : } \quad \bar{l} = 1 / \left(\frac{p_0}{mc_0^2} \right) \quad (2.14)$$

From these parameters it can be inferred that the solution of mass and momentum transport equations with different initial pressures lead to the same result for the same values of the dimensionless space and time variables. Many of the equations of this section have been directly expressed in dimensionless variables and their importance can be directly seen. Equations in dimensional form, e.g. equation (2.7), can be rewritten easily in dimensionless form. They can teach us some additional scale: e.g. starting with time and velocity scales one deduces the additional length scale from equation (2.7).

3. Analysis of finite differencing as used in SIMMER-II hydrodynamics

The numerical hydrodynamics of SIMMER-II has been developed from the method developed for the KACHINA-code /4/. This method itself goes back to the ICE-techniques /5/ for single phase fluids. Various forms of spatial differencing have been proposed in the original ICE paper. In SIMMER-II only two techniques for spatial differencing are implemented:

- Upwind (= donor cell) differencing
- Interpolated donor cell differencing

Interpolated donor cell differencing may lead to instabilities as explained e.g. by Stewart /6/. This fact is also made plausible by Fig. 4, where we show that negative densities can be convected by this method. Consequently only upwind differencing has been used in our SIMMER calculations for SNR-300 postdisassembly studies and only this method will be investigated in some detail in this paper. Our main aim is the detailed understanding of the gas/liquid interface for this particular numerical technique. In the following we explain how the simple equation for gas mass transport can be used to represent the behavior near the interface. We use the continuity equation for the "macroscopic" (= smear) gas density $\bar{\rho}$

$$\frac{\partial \bar{\rho}}{\partial t} + v \frac{\partial \bar{\rho}}{\partial x} = 0 \quad (3.1)$$

$\bar{\rho}$... macroscopic gas density
 v ... gas velocity

where the incompressibility condition $\frac{\partial}{\partial x} v = 0$ (justified for small velocities) has been used.

This gas transport equation has been simplified in many respects compared to SIMMER-II. However the terms relevant for our test problem have been retained.

To represent our test problem using equation (3.1) we take the following initial conditions for the macroscopic gas density

$$\bar{\rho}(x) = \begin{cases} \bar{\rho}_0 & x \leq 0 \\ 0 & x > 0 \end{cases} \quad (3.2)$$

Equation (3.2) represents initially a so-called "contact discontinuity" (pressures and normal velocities are continuous at the interface, only the density is discontinuous). In order to simulate the test problem we prescribe the velocity at the gas/liquid interface using the analytical solution for the boundary velocity $U(t)$ (cf. equation (2.5b)). Neglecting the space dependence of v near the interface in (3.1) we can use $U(t)$ instead of v . By this procedure we get a very good approximation of the gas velocity v because of its weak space dependence. This fact can be shown quantitatively using equations (2.7) to (2.9) and the data for the test problem given in section 2.

The solution of equation (3.1) is well known if the velocity v is constant. The exact solution for constant v is given by

$$\bar{\rho}(x,t) = \bar{\rho}_0(x - vt) \quad (3.3)$$

where $\bar{\rho}_0(x)$ represents the initial density profile. Equation (3.3) describes then the transport of a density wave which moves with constant velocity and a fixed profile. An initial step profile (3.2) will move without smearing effects according to (3.3).

Von Neumann formula for interface smearing

Upwind differencing of (3.1) leads to

$$(\bar{\rho})_j^{n+1} = (1 - \alpha^n) (\bar{\rho})_j^n + \alpha^n (\bar{\rho})_{j-1}^n \quad (3.4)$$

$(\bar{\rho})_j^n$... density at time t^n and position x_j

$\alpha^n = U^n \frac{\Delta t}{\Delta x}$... Courant number

$U^n = U(t^n)$... interface velocity at time step t^n ,
is supposed to be positive

Δt ... time step increment

Δx ... space step increment

In (3.1) we have used the interface velocity as explained above. α^n will be dependent on the time step and the mesh sizes used for space and time.

For the time independent (i.e. constant velocity) case a lot of studies have been performed. In one particular important study /7/ a formula developed by von Neumann for interface smearing caused by the upwind difference scheme (3.4) is presented. The initial conditions (3.2) are used to derive the width δx of the numerical mixing region.

$$\delta x = \sqrt{(1-\alpha) X(t) \Delta x} \quad (3.5)$$

α ... Courant number for constant velocity U

$X(t)$... position of the interface, initially $X(0) = 0$

Δx ... space step increment

The smearing described in (3.5) is solely due to the use of upwind differencing. The exact solution - given by (3.3) - exhibits no smearing at all. The von Neumann formula (3.5) has several important consequences which will be discussed in the following.

(1) δx can be made zero only for $\alpha = 1$, i.e. for $\Delta x = U\Delta t$. In SIMMER-II calculations the conditions $\alpha \ll 1$ has to be fulfilled in order to get convergent solutions (e.g. for the pressure iteration and for the partial implicit phase transition model very small time steps have to be chosen).

(2) δx is not directly dependent on the velocity, rather it depends on the integral:

$$X(t) = \int_0^t U dt'$$

This is an indication that (3.5) may be valid also in cases where U depends on the time. For our test example where we have an accelerated flow we will prove the validity of (3.5) by theoretical considerations (in this section) and by SIMMER-II calculations (in the next section).

- (3) It is very inefficient to make the mesh size smaller in order to calculate more accurate solutions at the interface. If one wants to double the precision of the solution one has to use a four times smaller mesh size. This is very prohibitive in particular for two- and three-dimensional calculations.

In the following we try to clarify the reasons for the artificial diffusion of the interface using the method of Hirt /6/ and Zhoukov /7/. We try also to specify under what conditions (3.5) is valid for non-constant velocities.

Application of the Hirt/Zhoukov method to calculate the numerical viscosity

The smearing of the interface is accompanied by an artificial, i.e. numerical viscosity which will be quantified with the help of the method of Hirt /8/ and Zhoukov /9/. In this method a differential equation is constructed from the finite difference equation through Taylor series expansion.

We expand the density $\bar{\rho}(x,t)$ in the form of a Taylor series about the value of $\bar{\rho}_j^n$ at time step t^n and location x_j :

$$\begin{aligned} \bar{\rho}(x,t) = & (\bar{\rho})_j^n + (\bar{\rho}_t)_j^n (t-t^n) + (\bar{\rho}_x)_j^n (x-x_j) \\ & + (\bar{\rho}_{tt})_j^n \frac{(t-t^n)^2}{2} + (\bar{\rho}_{xx})_j^n \frac{(x-x_j)^2}{2} \\ & + (\bar{\rho}_{xt})_j^n \frac{(t-t^n)(x-x_j)}{2} + \dots \end{aligned} \quad (3.6a)$$

which leads to

$$(\bar{\rho})_j^{n+1} = (\bar{\rho})_j^n + (\bar{\rho}_t)_j^n \Delta t + (\bar{\rho}_{tt})_j^n \frac{(\Delta t)^2}{2} + \dots \quad (3.6b)$$

$$(\bar{\rho})_{j-1}^n = (\bar{\rho})_j^n + (\bar{\rho}_x)_j^n (-\Delta x) + (\bar{\rho}_{xx})_j^n \frac{(\Delta x)^2}{2} + \dots \quad (3.6c)$$

Introducing expressions (3.6a,b,c) into equation (3.4) where we use the velocity U instead of the Courant number α results in the differential equation

$$\frac{\partial \bar{\rho}}{\partial t} + U \frac{\partial \bar{\rho}}{\partial x} = U \frac{\Delta x}{2} \frac{\partial^2 \bar{\rho}}{\partial x^2} - \frac{\Delta t}{2} \frac{\partial^2 \bar{\rho}}{\partial t^2} \quad (3.7)$$

We rewrite now the second derivative with respect to time using the original differential equation:

$$\begin{aligned} \frac{\partial^2}{\partial t^2} \bar{\rho} &= \frac{\partial}{\partial t} \left(-U \frac{\partial \bar{\rho}}{\partial x} \right) \\ &= -U \frac{\partial}{\partial x} \left(\frac{\partial \bar{\rho}}{\partial t} \right) - \frac{\partial U}{\partial t} \frac{\partial \bar{\rho}}{\partial x} \\ &= U^2 \frac{\partial^2 \bar{\rho}}{\partial x^2} + U \frac{\partial U}{\partial x} \frac{\partial \bar{\rho}}{\partial x} - \frac{\partial U}{\partial t} \frac{\partial \bar{\rho}}{\partial x} \end{aligned}$$

Now according to (2.5b)

$$\frac{\partial U}{\partial x} = 0 \quad \text{and} \quad \frac{\partial U}{\partial t} = a \left(= \frac{p_o}{m} \right)$$

and we get approximately

$$\frac{\partial^2}{\partial t^2} \bar{\rho} = U^2 \frac{\partial^2 \bar{\rho}}{\partial x^2} - a \frac{\partial \bar{\rho}}{\partial x} \quad (3.8)$$

Introducing (3.8) into (3.7) leads to

$$\begin{aligned} \frac{\partial \bar{\rho}}{\partial t} + \left(U + a \frac{\Delta t}{2} \right) \frac{\partial \bar{\rho}}{\partial x} &= U \frac{\Delta x}{2} \frac{\partial^2 \bar{\rho}}{\partial x^2} - \frac{\Delta t}{2} U^2 \frac{\partial^2 \bar{\rho}}{\partial x^2} \\ &= \frac{\partial^2 \bar{\rho}}{\partial x^2} \underbrace{\frac{U \Delta x - U^2 \Delta t}{2}}_{\mu} \end{aligned} \quad (3.9)$$

Equation (3.9) can now directly be compared to our original differential equation (3.1) and to the consequences of the von Neumann formula (3.5). We summarize the results of this comparison below.

- (1) At the right hand side of (3.9) there is an additional term representing the artificial diffusion of our upwind difference scheme. The quantity named μ is the artificial viscosity we wanted to compute. μ depends on the velocity U and on the space and time step sizes, for small time step sizes μ depends linearly on U . If U increases we expect an increased smearing in this case, a fact consistent to the von Neumann formula (3.5).
- (2) No artificial diffusion and no interface smearing is expected for $\mu = 0$, i.e.

$$U = \frac{\Delta x}{\Delta t}$$

This condition is identical to set $\alpha = 1$ in equation (3.4) and (3.5). The results of the Hirt/Zhoukov and the von Neumann formula are identical.

- (3) If $\mu < 0$ we have an "antidiffusive" term in equation (3.9). This will introduce instabilities in the difference scheme (3.4). The Hirt/Zhoukov method leads therefore to the well known stability criterion for (3.4), namely $\alpha \leq 1$ and is consistent with (3.5) where $\alpha > 1$ results in a pure imaginary smearing width δx .

- (4) An additional term $a \frac{\Delta t}{2} \frac{\partial \rho}{\partial x}$ is found at the left hand side of (3.9) compared to (3.1). This term is generated by the time dependence of U. As U is approximated very well by $U = at$, this additional term will perturb the equation only during the first few time steps. Afterwards it can be safely neglected. This finding corroborates the conjecture that the von Neumann formula works also for accelerated flow because a constant velocity U leads to an identical differential equation (3.9) except for few initial time steps.

In the next section we will verify these results by numerical experiments with SIMMER-II.

4. Discussion of SIMMER-II results and their relation to analytical solutions

In the following we discuss SIMMER-II results for our test problem in comparing them to analytical results. The SIMMER-II results obtained in this study used two different mesh sizes: 6 cm and 12 cm. To minimize the computing effort these mesh sizes have been applied only in the area of interest, however. Outside this area rather large mesh sizes have been introduced to simulate the semi-infinite spaces at the left and right hand side during the first few hundred milliseconds of expansion. The inside/outside transition has been carefully designed (avoiding abrupt mesh-size changes) in order to minimize numerical errors. A listing of the SIMMER-II input for a mesh size of 6 cm is reproduced in the Appendix.

In the following a short summary of the content of the present section is given.

Firstly, we discuss the interface smearing effects in SIMMER-II and show that they stem mainly from the donor cell differencing technique discussed in section 3. The exact location of the interface is given by the analytical solution (2.6). Detailed comparisons of SIMMER-II results to the von Neumann formula (3.5) for interface smearing, i.e. comparisons of the dependence on mesh size and on the location of the interface, verify that the von Neumann formula is directly applicable to SIMMER-II results and can also be used for accelerated flows. All the conclusions drawn from the von Neumann formula in section 3 remain therefore valid for the SIMMER-II solutions, in particular the conclusion that there is no efficient way to prevent interface smearing by mesh refinement.

Secondly, we compare SIMMER-II results for gas velocities and gas pressures to the analytical formulae developed in detail in section 2. Some irregularities - mainly in the smeared interface region - will be observed in SIMMER-II solutions. It is of interest that the finer mesh size of 6 cm does not always lead to a better representation of pressures and velocities.

Thirdly, we compare SIMMER-II results to the analytical results of section 2 for the conversion process of the internal energy of the gas to the kinetic energy of the liquid slug. It will be shown that the values of the kinetic energy can be calculated with high accuracy with the SIMMER-II code. This is in contrast to statements in a paper of Wirz /10/ where he argues that by numerical effects kinetic energy will be lost in SIMMER-II calculations. Also in opposition to /10/ is the finding that at the very early stage of the expansion process SIMMER-II predicts even too large values for the kinetic energy. However this amount of energy is negligible compared to the total kinetic energy generated during the later phases of the expansion.

Interface Smearing

Fig. 5 and Fig. 6 show the gas density distributions near the interface as calculated by SIMMER-II. The two mesh configurations mentioned above are used: Fig. 5 shows the results for a mesh width of 6 cm, Fig. 6 the results for a width of 12 cm. Three points of characteristic expansion times have been chosen for comparison: 100 ms, 160 ms and 200 ms. The results of the upwind scheme (3.4) are also shown. The velocity at the interface is taken from the analytical expression (2.5b). In these plots the exact location of the interface - given by (2.6) - is also indicated.

The following general conclusion can be drawn from Fig. 5 and Fig. 6:

- (1) SIMMER-II results and upwind differencing results are very similar at all times investigated. The most prominent differences are shown near pure gas and pure liquid regions. Upwind differencing results are not so exact near pure liquid regions whereas SIMMER-II results are not so exact near pure gas regions. The higher accuracy of SIMMER-II results near pure liquid regions is probably connected with the gas/liquid momentum coupling accounted for in SIMMER-II. This coupling is not simulated in the upwind difference calculations.
- (2) The exact interface position intersects the numerical density distribution curves just above 50 %.

The following items corroborate the applicability of the von Neumann formula (3.5) for our test example:

- (3) A comparison of results for expansion times 100 ms and 200 ms have been done, to show that the von Neumann formula can be used also for accelerated flows (as argued in section 3). In Table I we list the smeared density values adjacent to the 50 % value for the 6 cm mesh.

Expansion time t = 100 ms		Expansion time t = 200 ms	
Mesh Nr.	Normalized Density	Mesh Nr.	Normalized Density
42	.84	50	.80
43	.65	51	.72
44	.40	52	.62
45	.15	53	.48
		54	.34
		55	.23

Table I : Comparison of smearing for different expansion times (i.e. different interface locations). The mesh size is 6 cm.

The normalized macroscopic densities of the gas in the range $0.25 \leq \bar{\rho} \leq 0.75$ are used to calculate the smearing width δx . Linear interpolation is applied in Table I. As the interface moves according to the law:

$$X \sim \frac{a}{2} t^2$$

the interface smearing δx must obey

$$\delta x \sim t \quad (4.1)$$

For 100 ms we find from Table I $\delta x = 2.13$ cell sizes, for 200 ms $\delta x = 4.19$ cell sizes. The linearity expressed by formula (4.1) is very well represented for different positions of the interface. This validates our approximations done during the calculation of the artificial viscosity in section 3. Using theoretical arguments it was shown there that the von Neumann formula should be applicable also for accelerated flows.

- (4) The task remains to validate the von Neumann formula for different mesh cell sizes. SIMMER-II calculations have therefore been repeated for a mesh cell size of 12 cm. The results are shown in Table II. Using the procedure described in item 3 to calculate the smearing width we find for expansion time 200 ms:

$$\delta x^{(6 \text{ cm})} = 4.19 \text{ cell sizes}$$

$$\delta x^{(12 \text{ cm})} = 2.99 \text{ cell sizes}$$

The ratio

$$\frac{\delta x^{(12 \text{ cm})}}{\delta x^{(6 \text{ cm})}} = \frac{2.99 \times 12}{4.19 \times 6} = 1.427$$

6 cm cell size		12 cm cell size	
Mesh Nr.	Normalized density	Mesh Nr.	Normalized density
50	.80	34	.86
51	.72	35	.76
52	.62	36	.62
53	.48	37	.44
54	.34	38	.26
55	.23	39	.09

Table II : Comparison of smearing for different mesh sizes at expansion time 200 ms

is very near the theoretical value $\sqrt{2} = 1.414$ inferred from the von Neumann formula (3.5). The dependence δx on the mesh width is very well represented by (3.5). Sharp interfaces suffer therefore invariably by a very pronounced smearing. This smearing is connected with donor cell differencing and there is no effective way to impede this smearing.

It should be mentioned that also a calculation with a mesh cell size of 3 cm has been performed. The results of this calculation corroborate our conclusions that SIMMER-II smearing effects can be described by the von Neumann formula. As the mesh cell size of 3 cm is unrealistic small for a full reactor calculation we do not present the results in detail in this report.

Change of the Mass of the Liquid Slug

An additional case was calculated to check the validity of the von Neumann formula. In this case the mass of the sodium slug was only one tenth of the reference mass. Time and length scales change in this case according to the equations (2.12) to (2.14). The comparisons have been done in this case for equal slug displacements. Therefore

$$\frac{a_R}{2} t_R^2 \sim \frac{a_{1/10}}{2} t_{1/10}^2$$

R ... subscript für reference case

1/10 ... subscript for $\frac{1}{10}$ slug mass

It follows

$$t_R : t_{1/10} = \sqrt{a_{1/10}} : \sqrt{a_R} = \sqrt{\frac{p_0}{m_{1/10}}} : \sqrt{\frac{p_0}{m_R}} = \sqrt{\frac{m_R}{m_{1/10}}} = \sqrt{10}$$

δx in the von Neumann formula must be directly comparable for the reference case and the one tenth mass case for corresponding expansion times. In Table III the data for the reference case and the case with 1/10 mass of the liquid slug are given for corresponding expansion times of 200 ms and 63.8 ms, respectively. The mesh cell size is 12 cm in these cases.

A very good agreement has been found for the expansion times 100, 160 and 200 ms. As the values for 200 ms represent the most severe test only these are given in Table III. For this time the smearing width $\delta x_{1/10}$ of the 1/10 mass case is found by interpolation

$$\delta x_{1/10} = 3.05 \text{ cell sizes}$$

This is to be compared to the reference case where δx has the value 2.99 cell sizes.

Ref. case Expansion time: 200 ms		1/10 Slug mass case Expansion time: 63.8 ms	
Mesh Nr.	Normalized densities	Mesh Nr.	Normalized densities
34	.86	34	.84
35	.76	35	.74
36	.62	36	.60
37	.44	37	.45
38	.26	38	.24
39	.09	39	0.02

Table III : Comparison of smearing effects for different liquid slug masses. The comparison is done for equal slug displacements, i.e. for different expansion times. The mesh size is 12 cm in these cases.

The dependence of the smearing width δx on the Courant number α is very weak in the domain of interest. The reason for this stems from the fact that only $\sqrt{1-\alpha}$ appears in equation (3.5). But the value of α is very small for actual SIMMER-II calculations, always smaller than 0.01. Therefore $\sqrt{1-\alpha}$ is close to 1 in all cases. The accuracy of the interpolation procedure to calculate δx does not provide a possibility to investigate the very weak dependence on the parameter α in this domain. (The small Courant numbers are caused in our test example by the small time step increments used in SIMMER-II to calculate explicitly the movement of the gas/liquid interface. In real reactor applications very small time step sizes are enforced often by the phase transition model which uses a semi-explicit algorithm).

Flow Field Parameters: Gas Pressures and Velocities

In the following SIMMER-II results for gas pressures and velocities will be compared to the analytical solutions of section 2. The comparative results are plotted in Fig. 7 to Fig. 10.

At the expansion time of 100 ms the pressure and velocity fields are represented better by SIMMER-II results for the 12 cm mesh cell size. The pressures for the 6 cm mesh size are obviously too low (cf. Fig. 7), mainly at the front. These low pressures at the front cause too high gas velocities (cf. Fig. 8) in the interface region and in the adjacent pure gas region. The 12 cm results show the same tendency as the 6 cm results, but they are not so pronounced. At 200 ms the situation is reversed as shown in Fig. 9 and 10. Here the 6 cm SIMMER-II solution represents better the pressure and velocity fields. Initially there is therefore some calculational mechanism which distorts the 6 cm SIMMER-II solution more effectively. This mechanism is connected with the fact that the relative changes are larger in the gas volume fractions in the liquid mesh cells directly adjacent to the gas/liquid interface for the 6 cm mesh cell size. The calculation of the gas volume fraction is performed explicitly in SIMMER-II, a larger error in this volume fraction corresponds to a larger error in the pressure. Only when the flow is established and the interface is sufficiently smeared the mesh size of 6 cm leads to a more accurate solution behind the interface than the mesh size of 12 cm.

Kinetic Energy of the Liquid Slug

The time development of the kinetic energy of the liquid slug has been calculated analytically (2.10) and is shown in Fig. 11. The time dependence is dominated by the quadratic term in time. In Fig. 12 results of our SIMMER-II calculations are compared to the exact values of the kinetic energy. Because the differences are generally small only the relative deviations are displayed in this Figure. Larger deviations (about 18 % relative error) can be observed only at the early expansion time of 20 ms. In this early phase of expansion the gas pressure on the slug is overestimated by a special algorithm used in SIMMER-II. This algorithm does not allow losses of gas mass during the early acceleration of the

5. Summary, conclusions and suggestions for future work

A test example has been used to study the accelerated flow near a gas/liquid interface. Analytical solutions have been generated in form of series expansions for this example. These "exact" solutions have been compared in detail to the corresponding SIMMER-II solutions. In the following we present the main results:

- The smearing of the gas/liquid interface is caused mainly by the upwind (= donor cell) differencing technique used in SIMMER-II. The von Neumann formula represents this smearing very well, therefore only a weak dependence on the mesh size is observed and there is no effective way to impede the strong smearing effect by mesh refinement.
- Gas velocities and pressures do not agree very well with the exact solutions. Too low pressures in the interface region (caused by the inaccurate, explicit calculation of the gas volume fraction) are found to be mainly responsible for the too high gas velocities. One possible remedy is a closer binding of liquid and gas fields using a modified gas/liquid momentum transfer function. However for the present form of SIMMER-II this would mean a global change of momentum transfer, i.e. a change in regions with no interface problems. An extra study would be necessary to investigate the effects of globally changed momentum transfer.
- The kinetic energy of the liquid slug agrees very well with the exact value. This fact is important because the kinetic energy of liquid sodium generated during the postdisassembly expansion phase is traditionally taken as a figure of merit closely connected to the loading of the lid of the reactor vessel.

The structure of various gas/liquid interfaces during the postdisassembly phase is of importance for many physical effects, e.g. the mixing of liquid fuel and liquid sodium, the condensation of fuel, steel and sodium vapor, the entrainment of liquid sodium into the expanding bubble and the advance of liquid sodium into the cover gas space.

As long as strong numerical interface smearing occurs one has to be careful in modelling these (and other) physical phenomena. One example of inaccurate modelling effects in the "off the shelf" version of SIMMER-II is provided by condensation: hot liquid fuel may penetrate into the smeared interface and transfer heat to liquid sodium, thereby evaporating liquid sodium. The sodium vapor generated joins the vapor field which moves with higher velocity radially outward than the liquid field. Therefore the sodium vapor enters quickly the interface region with high (cold) liquid sodium content and the vapor condenses in one time interval. (The fact that the gas velocities are too high near the interface aggravates further the problem of too high condensation rates). A measure to avoid these consequences of smearing must be found if a realistic description of the role of sodium vapor is necessary. (A special procedure of some relevance for the postdisassembly phase is worked out in /12/). Other phenomena e.g. the fuel/sodium heat transfer can be controlled by a careful choice of SIMMER-II input parameters.

It should be pointed out that the smearing of the liquid interface in the cover gas region of an LMFBR during the postdisassembly expansion phase calculated with SIMMER-II is also determined by the von Neumann formula. This smearing leads to a relative early slug impact with reduced pressure spikes. However these spikes last longer compared to true single phase impact spikes (water hammer). It is not known if the impulse on the cover can be represented reasonably well by SIMMER-II calculations. These questions will be studied in more detail in the future in connection with SIMMER-II calculations of postdisassembly experiments for SNR-typical geometries performed at the Stanford Research Institute /13/.

Finally we want to explain briefly how the present study could be extended in the future. Using a similar one-dimensional geometry as in the present report one could add in SIMMER-II studies gradually the effects of heat transfer, condensation and evaporation using hot materials in the bubble. Such a study can show

- (1) The influence of the interface smearing effects.
- (2) The measures to be taken to calibrate or change SIMMER-II models in order to bring them nearer to realism.

The findings of these SIMMER-II studies should be compared to the predictions of other codes and to experimental results.

In order to verify the modelling in the particular area of the post-disassembly expansion phase the existing and relevant experimental material has to be looked through and the useful data (including of course simulants) has to be compared to SIMMER-II predictions. SIMMER-II should be applied to a broad range of physical conditions which show in some respect resemblance to the postdisassembly phase. Proceeding in this manner will lead to a better understanding of the physical domain where we can rely on SIMMER-II predictions.

References

- /1/ L. L. Smith et al.:
"SIMMER-II: A Computer Program for LMFBF Disrupted Core Analysis"
NUREG/CR-0453; LA-7515-M, Rev. (1980)
- /2/ L. D. Landau and E. M. Lifshitz:
"Fluid Mechanics", Vol. 6 of Course of Theoretical Physics,
Chapter X, Pergamon Press (1963)
- /3/ W. I. Smirnov:
"Lehrgang der höheren Mathematik", Teil I
VEB Deutscher Verlag der Wissenschaften, Berlin (1956)
- /4/ A. A. Amsden and F. H. Harlow:
"KACHINA: An Eulerian Computer Program for Multifield Fluid Flows"
LA-5680 (1974)
- /5/ F. H. Harlow and A. A. Amsden:
"A Numerical Fluid Dynamics Calculation Method for All Flow Speeds",
J. Comp. Phys. 8, 197 (1971)
- /6/ H.'B. Stewart: private communication (1980)
- /7/ A. Blair et al.:
"A Study of a Numerical Solution to a Two-Dimensional Hydrodynamical
Problem", Math. Tables and Other Aids to Computation 13, 145 (1959)
- /8/ C. W. Hirt:
"Heuristic Stability Theory for Finite Difference Equations"
J. Comp. Phys. 2, 339 (1968)
- /9/ Zhukov: cited in G. I. Marchuk:
"Methods of Numerical Mathematics", p. 236, Springer Verlag, New York-
Heidelberg-Berlin (1975)

/10/ H. J. Wirz:

"On some problems in two- and single phase flows", undated report,
written for the Commission of the European Communities under Contract
No. 466-78-10 ECI B.

/11/ C. R. Bell et al.:

"Impact of SIMMER-II Model Uncertainties on Predicted Postdisassembly
Dynamics", NUREG/CR-1058, LA-8053-MS (1979)

/12/ P. Schmuck: to be published

/13/ R. Tobin: private communication (1981)

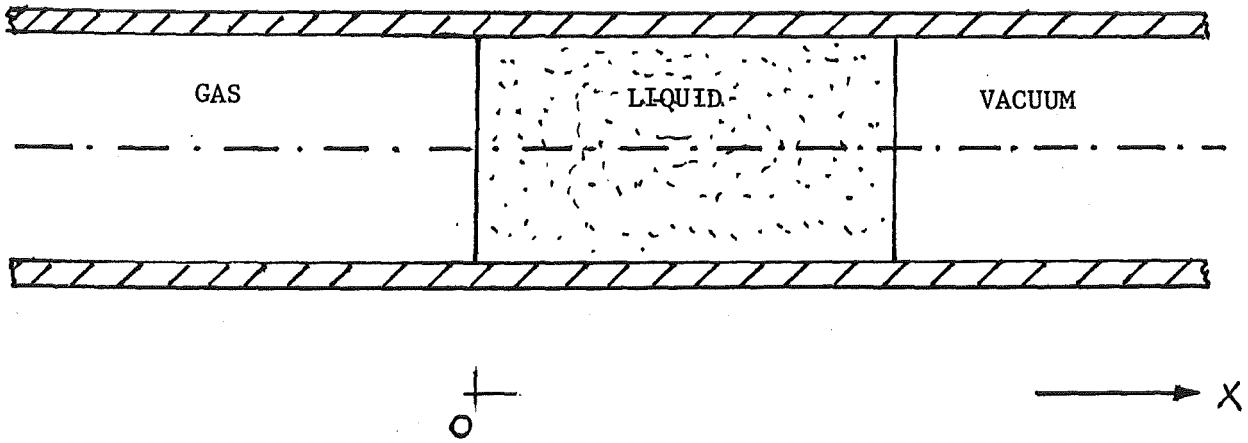


Fig. 1: Geometry of the test problem: Initial distribution of gas, liquid and vacuum in a cylindrical tube

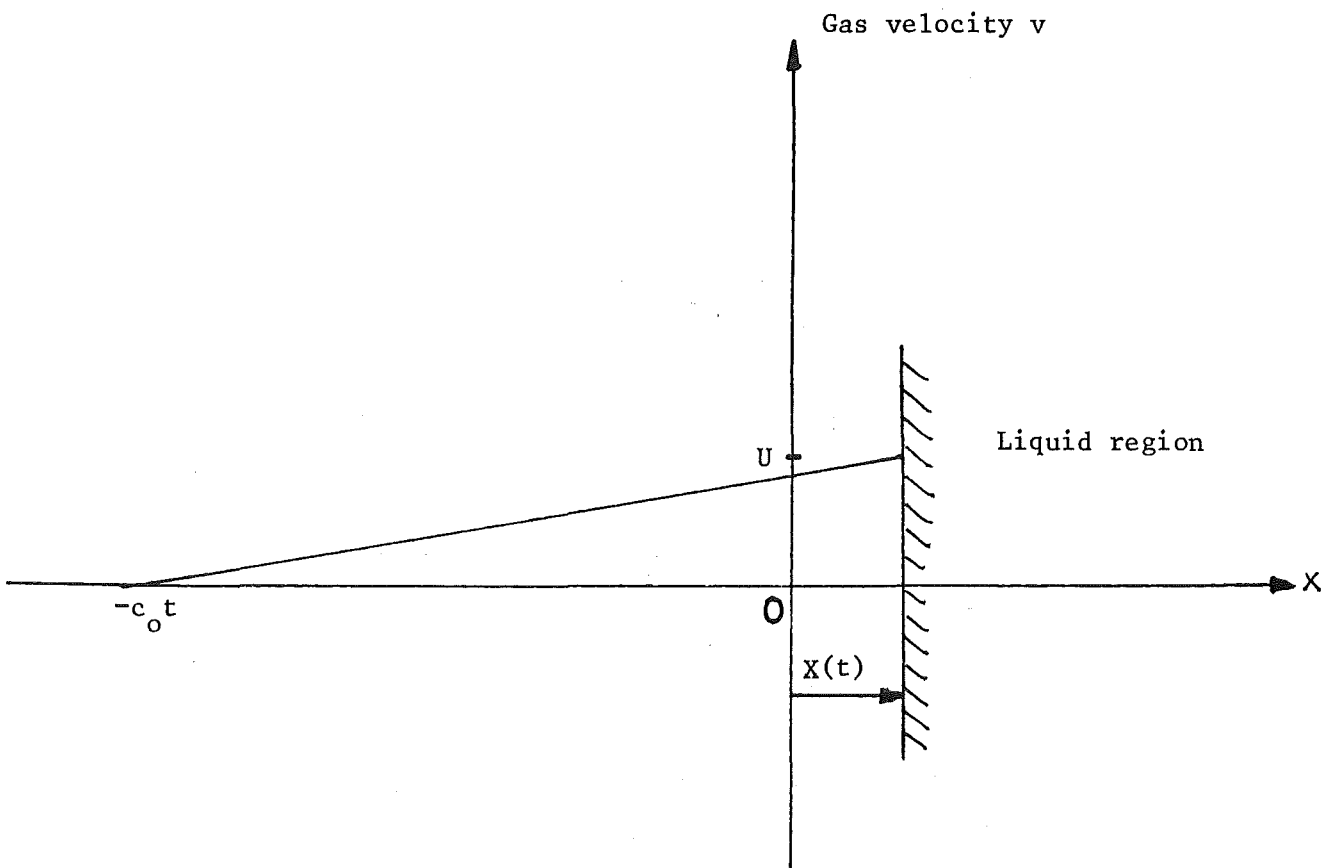


Fig. 2: Schematic sketch of the velocity distribution of the gas at time t between the liquid slug and the gas masses at rest (U is the slug velocity, $X(t)$ the slug displacement, c_0 the velocity of sound in the gas at rest)

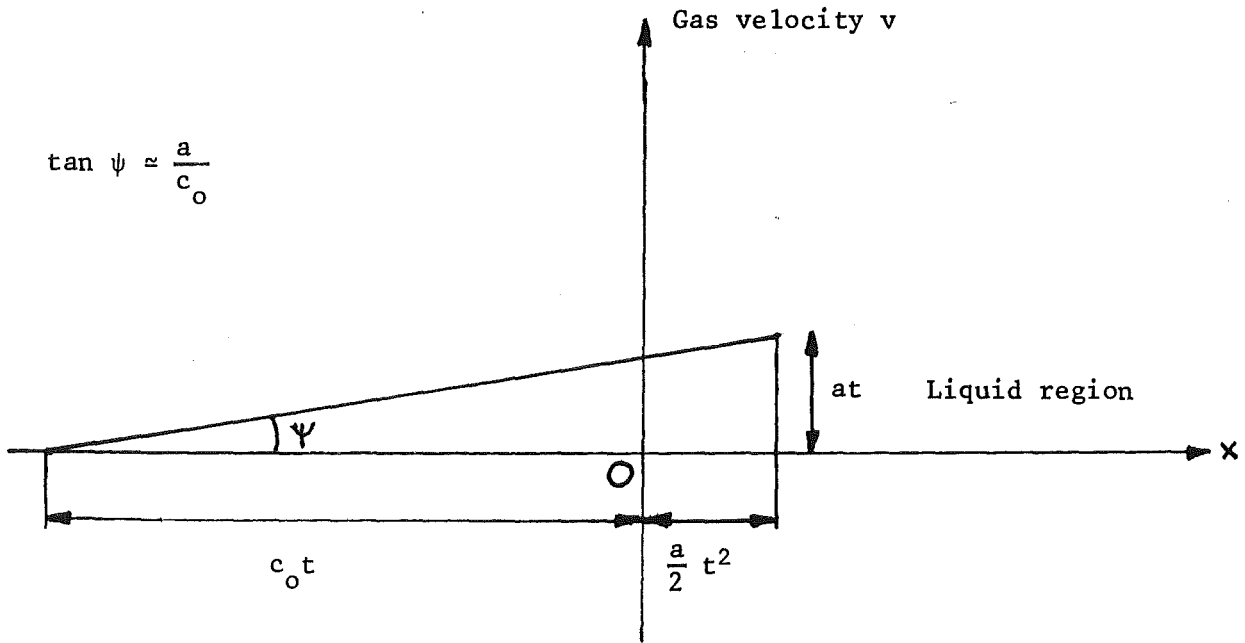


Fig. 3: Important quantities determining the space dependence of the gas velocity for a uniformly accelerated liquid slug (slug velocity $U = at$)

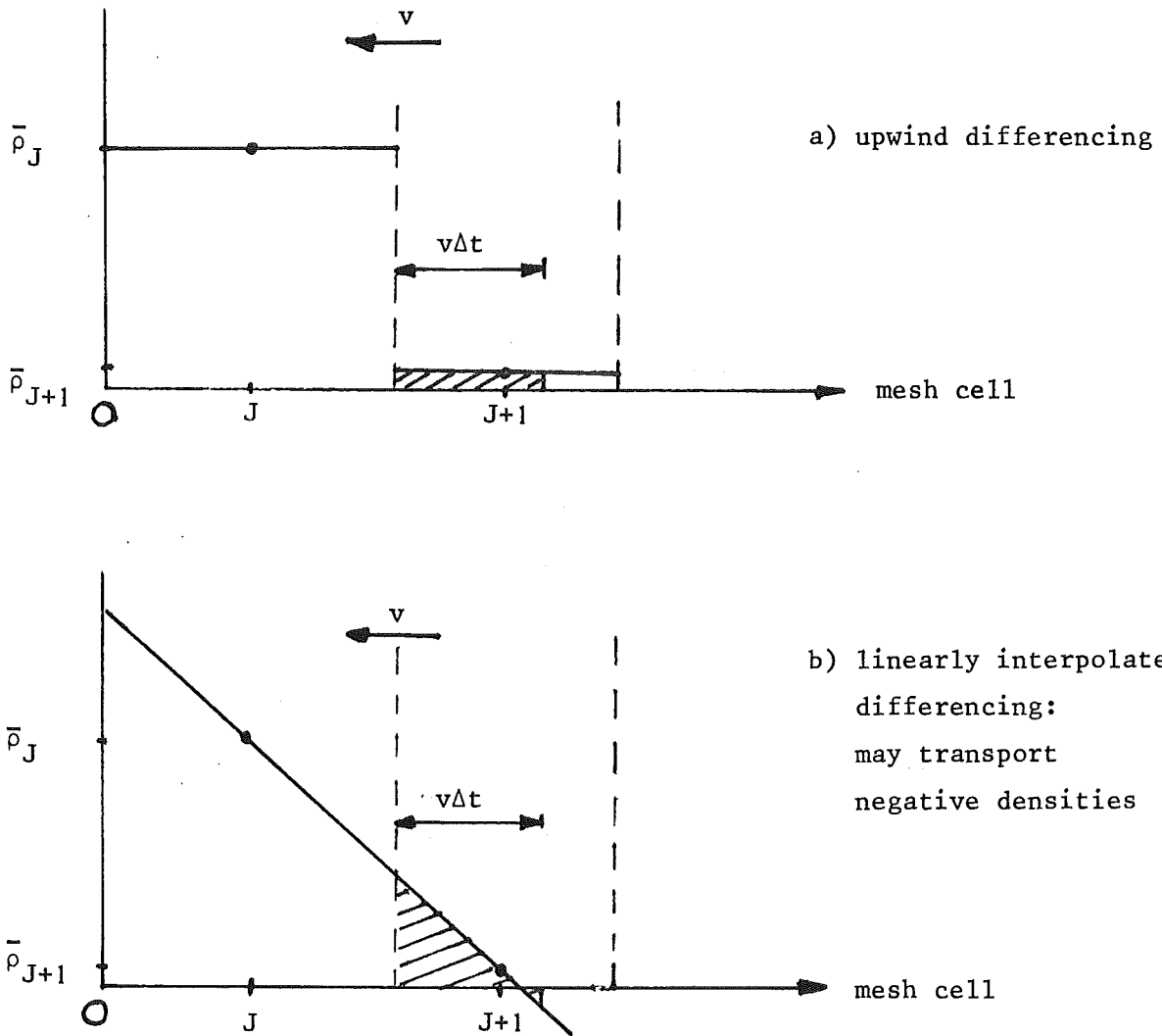


Fig. 4: Axial convection of the gas mass at mesh interface $j + 1/2$
(v is the gas velocity, $\bar{\rho}$ the macroscopic density)

a) upwind (donor cell) differencing:

$$A_o = 1/2, B_o = 0 \text{ in SIMMER-II}$$

b) linearly interpolated differencing:

$$A_o = 0, B_o = 1/2 \text{ in SIMMER-II}$$

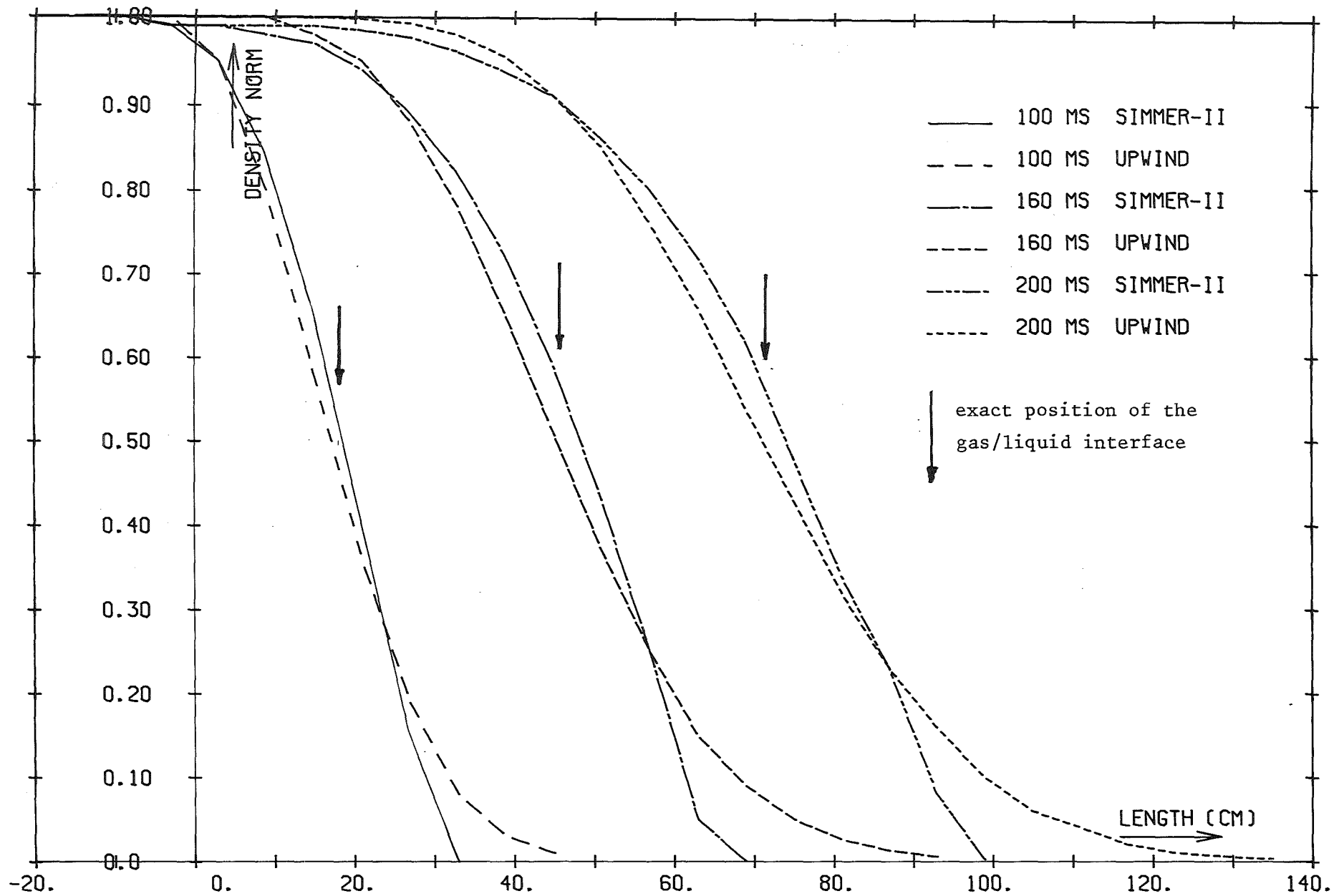


FIG. 5 TIME DEVELOPMENT OF A STEP PROFILE IN GAS DENSITY-6CM MESH

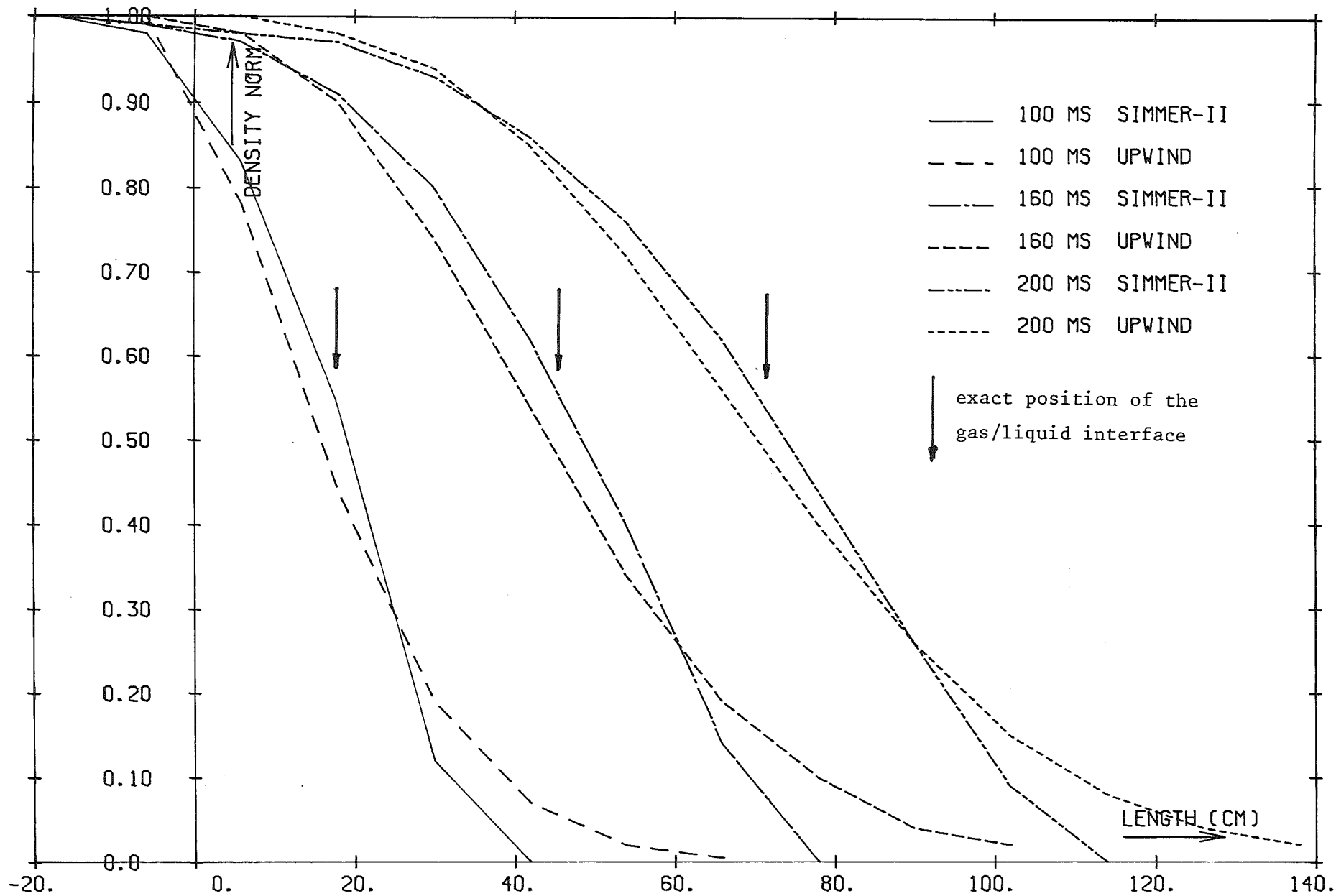


FIG. 6 TIME DEVELOPMENT OF A STEP PROFILE IN GAS DENSITY-12CM MESH

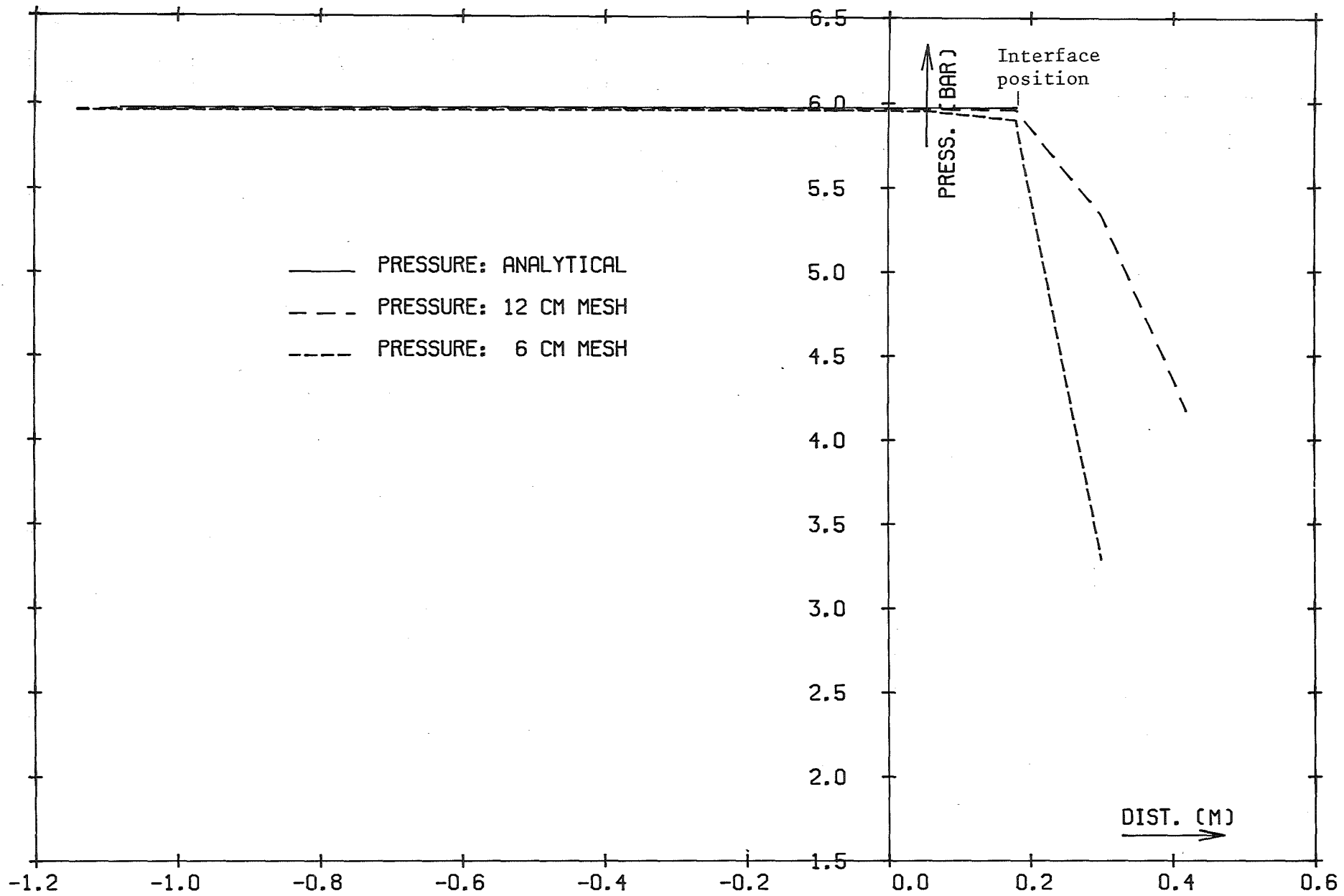


FIG. 7 GAS PRESSURE DISTRIBUTION (100 MS)

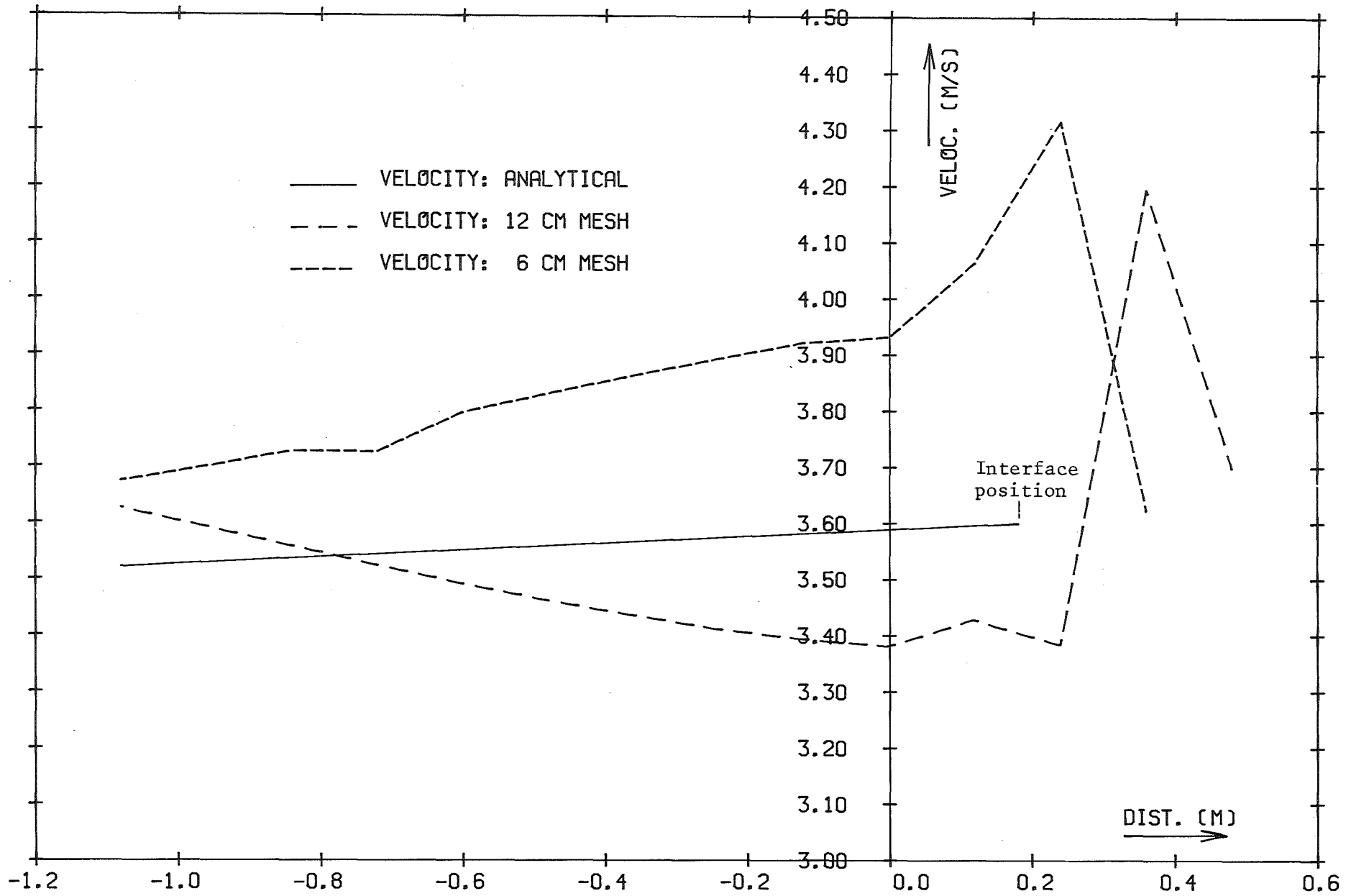


FIG. 8 GAS VELOCITY DISTRIBUTION (100 MS)

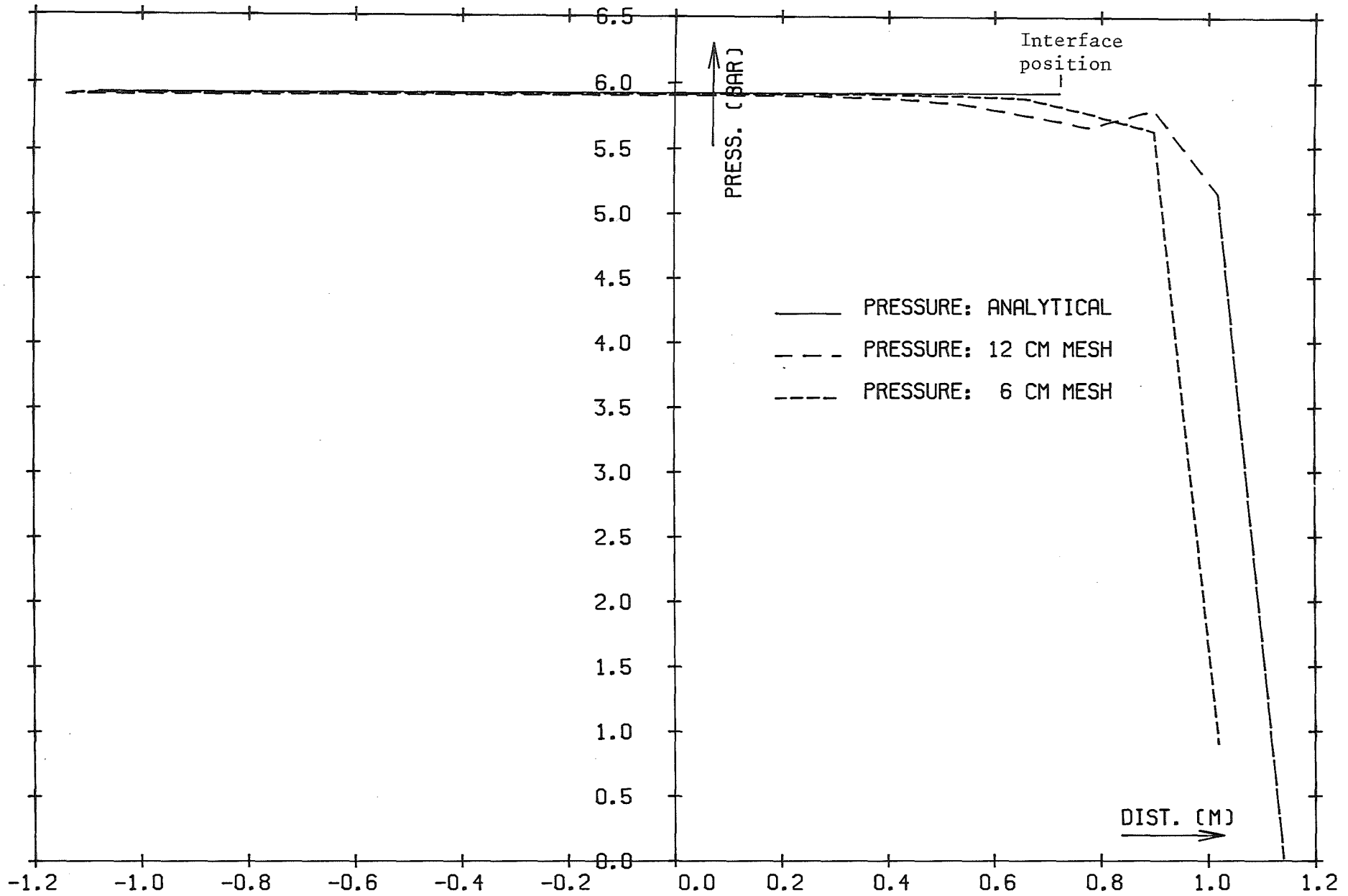


FIG. 9 GAS PRESSURE DISTRIBUTION (200 MS)

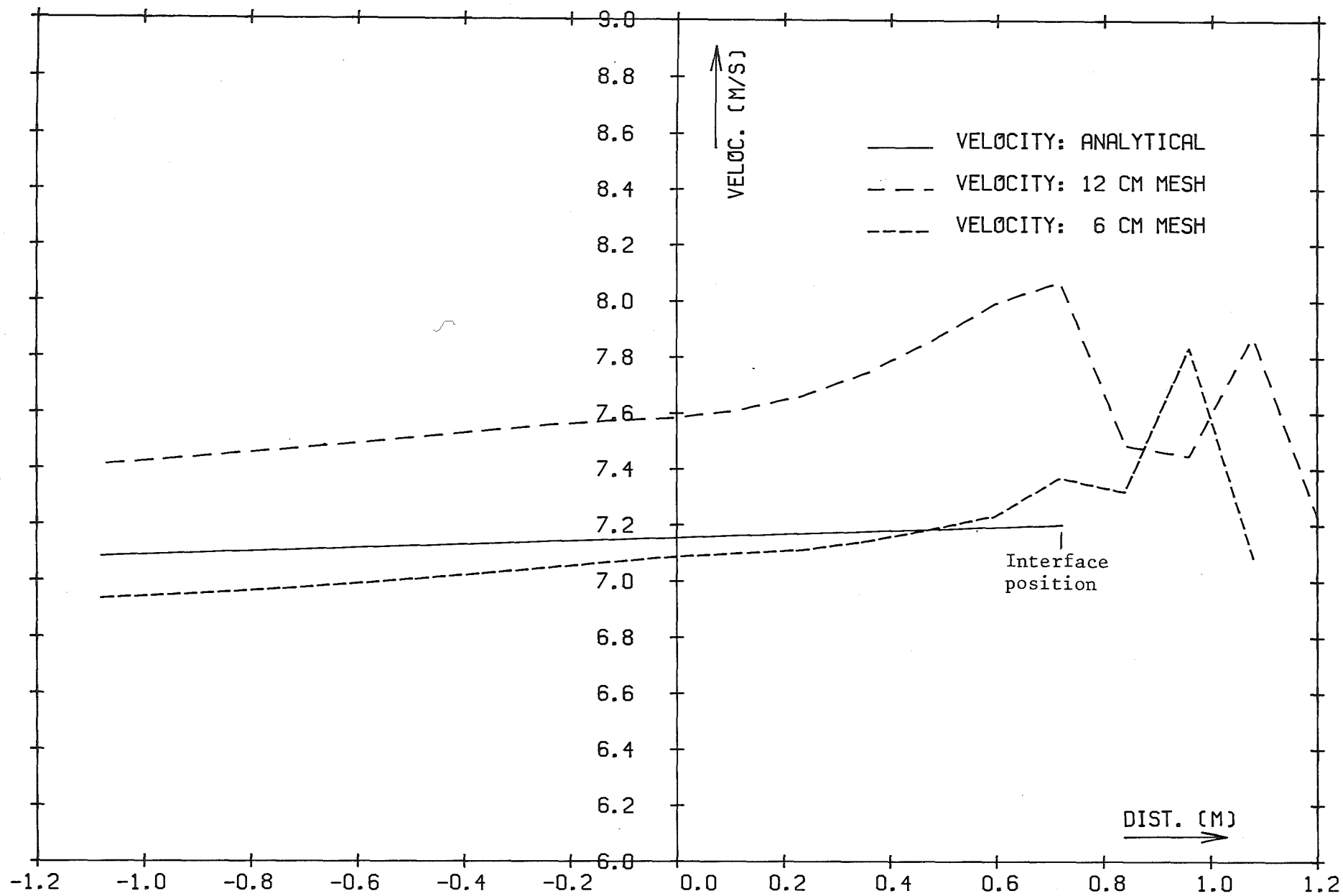


FIG. 10 GAS VELOCITY DISTRIBUTION (200 MS)

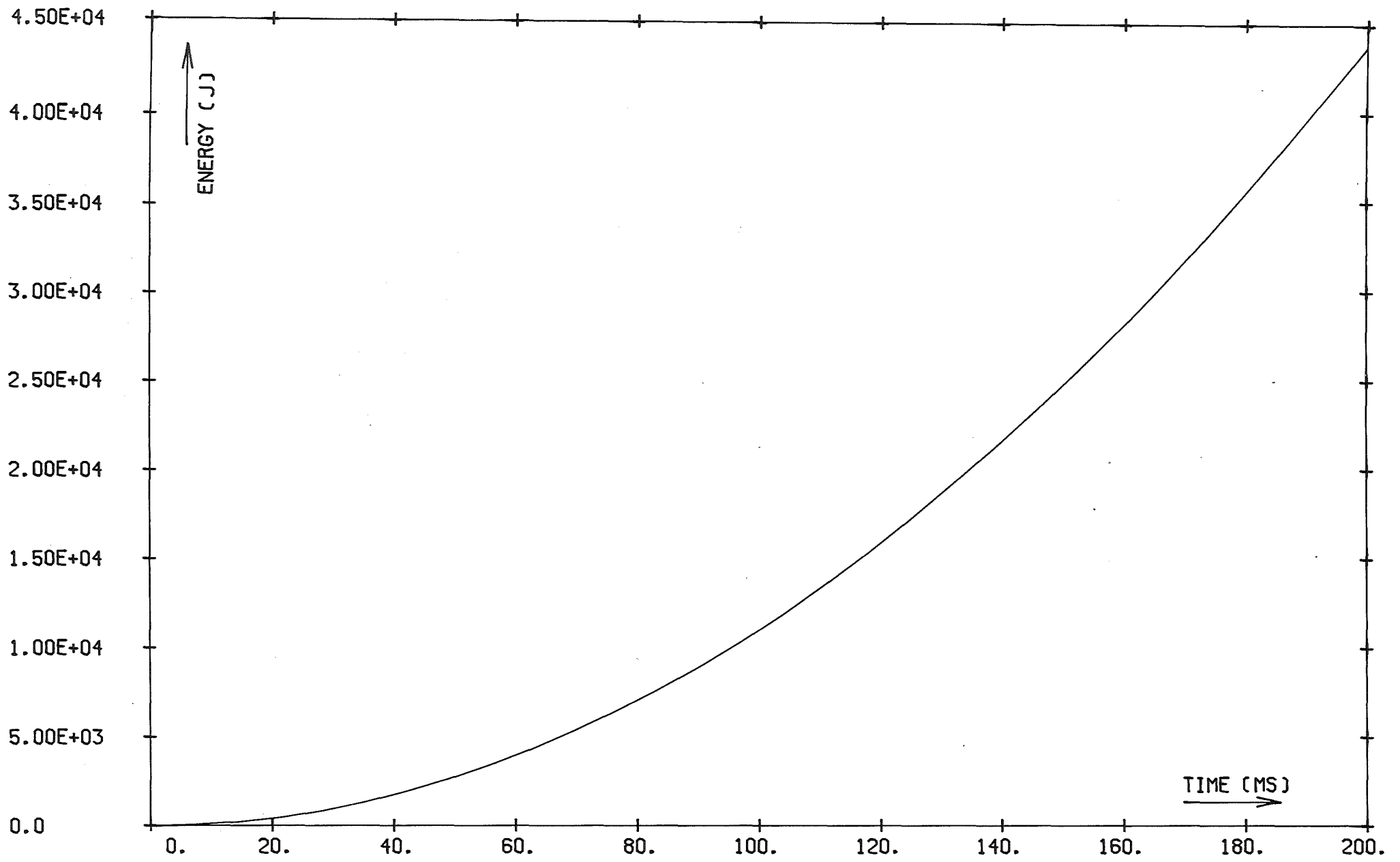


FIG. 11 KINETIC ENERGY FOR THE PISTON PROBLEM (ANALYTIC CALCULATION)

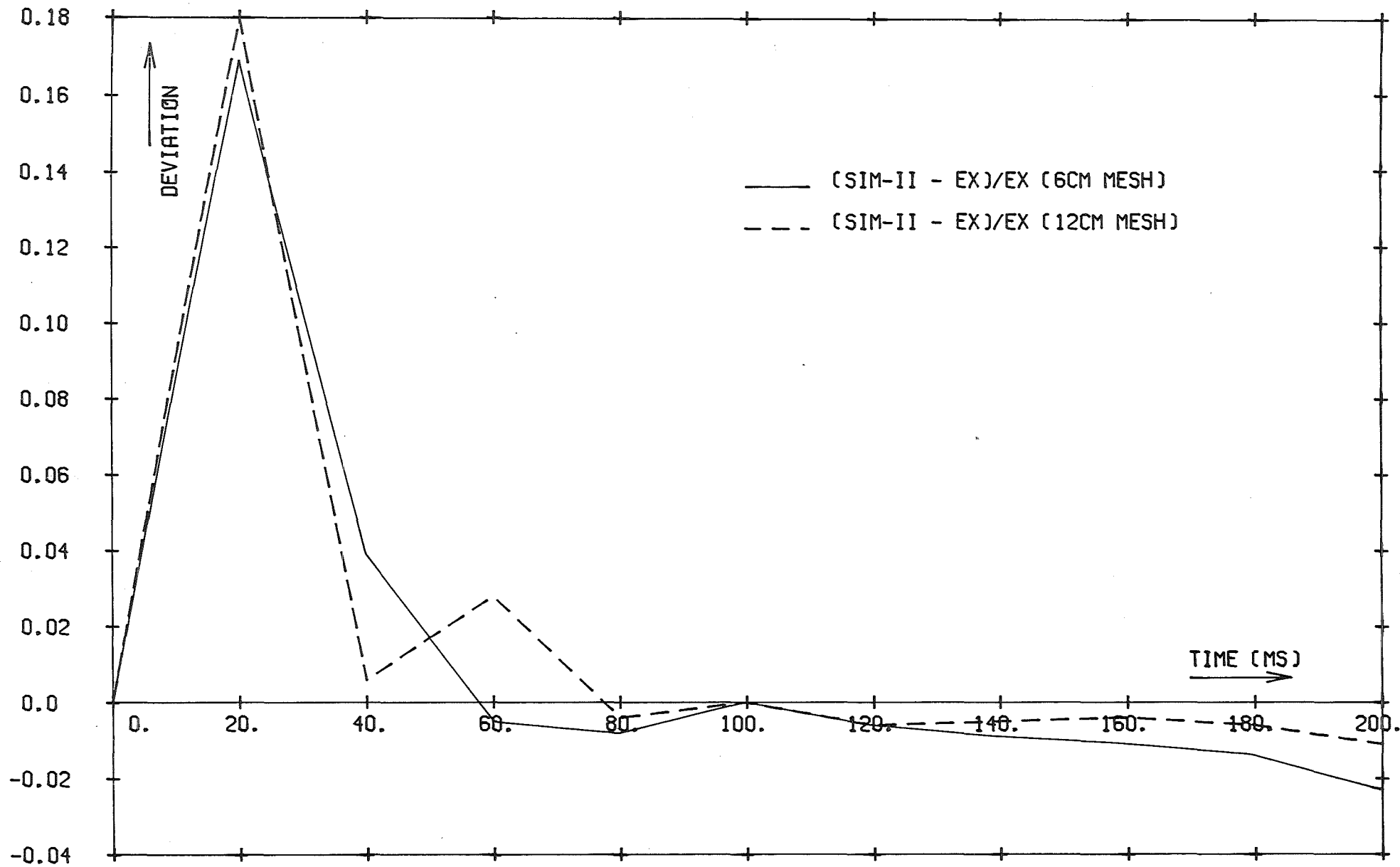


FIG. 12 DEV. OF SIMMER-II RESULTS FROM EXACT KINETIC ENERGY VALUES

A P P E N D I X

Typical SIMMER-II input data for a case with the mesh cell size of 6 cm are listed on the following pages. An additional second row of meshes has been introduced in radial direction in order to test whether the formulation of boundary conditions in SIMMER-II (free slip boundary conditions in this case) can influence the solutions or whether other numerical effects can produce non-symmetric solutions. It was found that the boundary conditions were correctly formulated and no influence on the solutions could be observed. Also non-symmetries were not detected in the solutions.

0.0										00540000
0.0										00550000
0.0										00560000
0.0										00570000
0.0										00580000
0.0										00590000
VIEW FACTORS										00600000
										00610000
TIME STEP CONTROLS										00620000
0.0	1.00000E-06	1.00000E-10	0.3							00630000
0.001	0.25	1.0	0.1		1.0		1.0			00640000
5.42500E+06	0.96	0.02	0.02		0.0			1.E-10		00650000
STRUCTURE AND FAILURE PARAMETERS										00660000
	.9	.9	.5		0.		0.			00670000
	0.									00680000
	1.	1.	.51		1.		1.			00690000
	3.E+6	1.E+6	7.E+5		8.E+5		9.E+5		2.E+3	00700000
	3.E+4	9.E+3	2.E+1							00710000
FUEL PROPERTIES AND EQUATION OF STATE										00720000
9890.0	638.0	3100.0		2.76000E+05	2.0					00730000
8580.0	504.0	0.45		2.5	4.30000E-03					00740000
1.44000E+11	5.17080E+04	0.0		2.62000E+06	8400.0		0.597			00750002
511.0	1.05			4.4	0.00000E+08	270.0	6508.			00760000
	0.0	0.0								00770000
STEEL PROPERTIES AND EQUATION OF STATE										00780002
7365.00	639.0	1700.0		2.60000E+05	25.0					00790002
6100.0	650.0	1.6		20.0	5.36000E-03					00800000
1.33800E+11	4.33700E+04	0.0		8.17000E+06	10000.0		0.360			00810000
492.0	1.26			1.64	0.00000E+09	56.0	7700.			00820000
	0.0	0.0								00830000
SODIUM PROPERTIES AND EQUATION OF STATE										00840000
0.0										00850002
705.000E+01	1300.0	0.1		50.0	1.50000E-04					00860000
3.76000E+09	1.21300E+04	10.0		4.81600E+06	2503.0		0.341			00870002
1500.0	1.65			3.567	0.00000E+07	23.0	1365.			00880000
	0.0	0.0								00890000
CONTROL MATERIAL PROPERTIES AND EQUATION OF STATE										00900000
2520.0	1893.0	2623.0		2.50000E+05	83.74					00910000
2520.0	1890.0	1.0		80.0	1.00000E-03					00920000
4.28600E+14	8.36800E+04	0.0		5.00000E+06	7107.0		0.350			00930002
500.0	1.50			1.50	0.00000E+09	65.3	5472.			00940000
	0.0	0.0								00950000
FISSION GAS PROPERTIES AND EQUATION OF STATE										00960000
0.0										00970000
0.0										00980000
1.00000E+11	4.00000E+04	0.0		5.00000E+06	126.2	0.3				00990000
	727.0	1.400000		3.80	0.00E+6	28.	71.4			01000000
	0.0	0.0								01010000
COMPONENT PROPERTIES										01020002
9890.0	9890.0	9890.0		9890.0	7365.0	7365.0				01030000
2520.0	0.0									01040002
8580.0	8580.0	6100.0		705.000E+01	2520.0	9890.0				01050002
9890.0	7365.0	0.0								01060000
2.00000E+03	2.00000E+03	2.00000E+03		2.00000E+03	2.00000E+03	2.00000E+03	2.00000E+03	2.00000E+03	2.00000E+03	01060000

2.00000E+03	2.00000E+03	2.00000E+03					01070000
HEAT TRANSFER CORRELATION DATA							01080000
0.2	100.	1.	1.	1.	1.	1.	1.01090000
1.	1.	1.	1.	1.	1.	1.	1.01100000
1.	1.	1.	1.	1.	1.	1.	01110000
0.023	0.8	0.4	0.				01120000
0.023	0.8	0.4	5.				01130000
0.023	0.8	0.4	5.				01140000
0.023	0.8	0.4	0.				01150000
0.023	0.8	0.4	0.				01160000
.687	0.673	0.33	2.0				01170000
DRAG CORRELATION DATA							01180000
100.0	22.0	2.0E-4	9.2E-7		1.0		01190000
2.5	1.	0.5					01200000
0.050	-0.2	0.001	0.050		-0.2		0.00101210000
PARAMETER REGION 1 (CORE REGION)							01220000
1.	0.	1.E5	0.002545		0.002545		0.002801230000
236.	0.	32.	0.31		0.0		0.1101240000
0.00789	0.00789	0.105	2.62E3		0.0		1.79E401250000
1950.0	0.68	1.00000E+05	2.30000E-05		1.00000E-17		1.00000E-0301260000
1.0E-5							01270000
PARAMETER REGION 2 (BLANKET REGION)							01280000
1.	0.11	1.E5	0.002545		0.003		0.002801290000
236.	278.	32.	0.31		0.10		0.1101300000
0.00533	0.00789	0.105	2.62E3		1.32E5		1.79E401310000
1950.0	0.68	1.00000E+05	2.30000E-05		1.00000E-17		1.00000E-0301320000
1.0E-5							01330000
PARAMETER REGION 3 (MIXING HEAD REGION)							01340000
3.	.08	1.E5	0.		1.5E-4		0.0101350000
0.	16.	24.	0.		0.14		0.1801360000
1.5E-2	0.09	0.09	0.		5.E3		5.E301370000
1950.0	0.68	1.00000E+05	2.30000E-05		1.00000E-17		1.00000E-0301380000
1.0E-5							01390000
PARAMETER REGION 4 (EXIT REGION)							01400000
5.	.2	1.E5	0.		0.		0.002801410000
0.	0.	32.	0.		0.		0.1101420000
0.105	0.105	0.105	0.		0.		1.79E401430000
1950.0	0.68	1.00000E+05	2.30000E-05		1.00000E-17		1.00000E-0301440000
1.0E-5							01450000
PARAMETER REGION 5 (REFLECTORS, SHIELD TANK ETC)							01460000
5.	0.	1.E5	0.		0.		0.0501470000
		32.			.8700407332		.1100 01480000
0.0025	0.0025	0.0025	1.79E4		1.79E4		1.79E401490000
1950.0	0.68	1.00000E+05	2.30000E-05		1.00000E-17		1.00000E-0301500000
1.0E-5							01510000
PARAMETER REGION 6 (PERFORATED DIP PLATE)							01520000
3.	0.051	1.E5	0.		0.03		0.002801530000
	100.	32.			0.59		.129 01540000
0.059	0.059	0.059	0.		1.E3		1.E301550000
1950.0	0.68	1.00000E+05	2.30000E-05		1.00000E-17		1.00000E-0301560000
1.0E-5							01570000
PARAMETER REGION 7 (SODIUM POOL)							01580000
7.	0.	1.E5	0.0		0.0		0.001590000

										01600000
1950.0	1.	1.	1.	0.0	0.0	0.001610000				0.001610000
	0.68		1.00000E+05	2.30000E-05	1.00000E-17	1.00000E-03	01620000			01620000
	1.0E-5						01630000			01630000
PARAMETER	REGION	8	(HOLE IN DIP PLATE SUPPORT STRUCTURE)				01640000			01640000
	5.	0.	1.E5	0.0	0.0	0.1001650000				0.1001650000
	0.	0.	1.	0.0	0.0	0.8801660000				0.8801660000
	0.125	0.125	0.125	0.0	0.0	5.E201670000				5.E201670000
1950.0	0.68		1.00000E+05	2.30000E-05	1.00000E-17	1.00000E-03	01680000			01680000
	1.0E-5						01690000			01690000
PARAMETER	REGION	9	(CORE REGION WITH INTACT CLADDING)				01700000			01700000
	1.	0.11	1.E5	0.002545	0.003	0.002801710000				0.002801710000
	236.	278.	32.	0.31	0.10	0.1101720000				0.1101720000
	0.00533	0.00789	0.105	2.62E4	1.32E5	1.79E401730000				1.79E401730000
1950.0	0.68		1.00000E+05	2.30000E-05	1.00000E-17	1.00000E-03	01740000			01740000
	1.0E-3						01750000			01750000
VAPOR AND LIQUID VELOCITIES ON THE BOTTOM BOUNDARY										01760000
HIGH PRESSURE SPACE										01770000
	1	40	1	2	3	1	0	0	8	01780000
										01790000
										01800002
										.007 01810000
										01820000
										800. 01830000
										0.07 01840000
										01850000
										800.0 01860000
										3.00E-3 2.58 01870000
										01880000
										800. 01890000
0.0	0.0	0.0	0.0	0.0	0.0001	0.001				01900000
LIQUID SLUG REGION	(HIGH DENSITY SODIUM)									01900000
	41	80	1	2	3	1	0	0	8	01910002
										.007 01920000
										01930000
										800. 01940000
										690.893E+1 01950002
										01960000
										800. 01970000
										0.004 .930 01980000
										01990000
000.	800.	000.	0.0	0.0	0.0001	0.001				02000000
COVER GAS SPACE										02010000
	81	100	1	2	3	1	0	0	8	02020004
										.007 02030000
										02040000
										800. 02050000
										0.07 02060000
										02070000
										800.0 02080000
										3.00E-3 0.007 02090000
										02100000
0.0	800.	0.0	0.0	0.0	0.0001	0.001				02110000